

Submit a Manuscript: <https://www.f6publishing.com>*World J Gastroenterol* 2023 February 14; 29(6): 1076-1089

DOI: 10.3748/wjg.v29.i6.1076

ISSN 1007-9327 (print) ISSN 2219-2840 (online)

ORIGINAL ARTICLE

Retrospective Study**Clinical-radiomics nomogram for predicting esophagogastric variceal bleeding risk noninvasively in patients with cirrhosis**

Rui Luo, Jian Gao, Wei Gan, Wei-Bo Xie

Specialty type: Gastroenterology and hepatology**Rui Luo, Jian Gao**, Department of Gastroenterology and Hepatology, The Second Affiliated Hospital of Chongqing Medical University, Chongqing 400010, Chongqing, China**Provenance and peer review:**

Unsolicited article; Externally peer reviewed.

Wei Gan, Wei-Bo Xie, Department of Radiology, The Second Affiliated Hospital of Chongqing Medical University, Chongqing 400010, Chongqing, China**Peer-review model:** Single blind**Corresponding author:** Jian Gao, MMed, PhD, Chief Doctor, Professor, Department of Gastroenterology and Hepatology, The Second Affiliated Hospital of Chongqing Medical University, No. 76 Linjiang Road, Yuzhong District, Chongqing 400010, Chongqing, China. gaojian@cqmu.edu.cn**Peer-review report's scientific quality classification**

Grade A (Excellent): 0

Grade B (Very good): B, B

Grade C (Good): C, C

Grade D (Fair): D

Grade E (Poor): 0

P-Reviewer: Chen SH, Taiwan; Paparoupa M, Germany; Tai DL, Taiwan**Abstract****BACKGROUND**

Esophagogastric variceal bleeding (EGVB) is a serious complication of patients with decompensated cirrhosis and is associated with high mortality and morbidity. Early diagnosis and screening of cirrhotic patients at risk for EGVB is crucial. Currently, there is a lack of noninvasive predictive models widely available in clinical practice.

AIM

To develop a nomogram based on clinical variables and radiomics to facilitate the noninvasive prediction of EGVB in cirrhotic patients.

METHODS

A total of 211 cirrhotic patients hospitalized between September 2017 and December 2021 were included in this retrospective study. Patients were divided into training ($n = 149$) and validation ($n = 62$) groups at a 7:3 ratio. Participants underwent three-phase computed tomography (CT) scans before endoscopy, and radiomic features were extracted from portal venous phase CT images. The independent sample t-test and least absolute shrinkage and selection operator logistic regression were used to screen out the best features and establish a radiomics signature (RadScore). Univariate and multivariate analyses were performed to determine the independent predictors of EGVB in clinical settings. A noninvasive predictive nomogram for the risk of EGVB was built using independent clinical predictors and RadScore. Receiver operating characteristic, calibration, clinical decision, and clinical impact curves were applied to evaluate the model's performance.



RESULTS

Albumin ($P = 0.001$), fibrinogen ($P = 0.001$), portal vein thrombosis ($P = 0.002$), aspartate aminotransferase ($P = 0.001$), and spleen thickness ($P = 0.025$) were selected as independent clinical predictors of EGVB. RadScore, constructed with five CT features of the liver region and three of the spleen regions, performed well in training (area under the receiver operating characteristic curve (AUC) = 0.817) as well as in validation (AUC = 0.741) cohorts. There was excellent predictive performance in both the training and validation cohorts for the clinical-radiomics model (AUC = 0.925 and 0.912, respectively). Compared with the existing noninvasive models such as ratio of aspartate aminotransferase to platelets and Fibrosis-4 scores, our combined model had better predictive accuracy with the Delong's test less than 0.05. The Nomogram had a good fit in the calibration curve ($P > 0.05$), and the clinical decision curve further supported its clinical utility.

CONCLUSION

We designed and validated a clinical-radiomics nomogram able to noninvasively predict whether cirrhotic patients will develop EGVB, thus facilitating early diagnosis and treatment.

Key Words: Liver cirrhosis; Variceal bleeding; Radiomics; Nomogram; Diagnosis

©The Author(s) 2023. Published by Baishideng Publishing Group Inc. All rights reserved.

Core Tip: Esophagogastric variceal bleeding (EGVB) is a life-threatening complication of liver cirrhosis. Currently, no noninvasive prediction models for bleeding risk are widely used in clinical practice. Our study extracted radiomics features from computed tomography and identified portal vein thrombosis, fibrinogen, aspartate aminotransferase, albumin, and spleen thickness as independent clinical predictors. Consequently, we established a novel clinical-radiomics model for noninvasive prediction of EGVB. This model exhibits superior diagnostic performance and can assess bleeding risk early. It has the potential to facilitate early prevention and treatment of possible bleeding in cirrhotic patients with esophagogastric varices.

Citation: Luo R, Gao J, Gan W, Xie WB. Clinical-radiomics nomogram for predicting esophagogastric variceal bleeding risk noninvasively in patients with cirrhosis. *World J Gastroenterol* 2023; 29(6): 1076-1089

URL: <https://www.wjgnet.com/1007-9327/full/v29/i6/1076.htm>

DOI: <https://dx.doi.org/10.3748/wjg.v29.i6.1076>

INTRODUCTION

In liver cirrhosis, esophagogastric variceal bleeding (EGVB) is among the most common complications associated with portal hypertension, characterized by acute life-threatening sequelae and high mortality rates[1]. Approximately 50% of patients with cirrhosis develop esophagogastric varices (EGV) and approximately 10%–15% of these rupture and hemorrhage annually. Almost 12% – 20% of patients die within 6 wk of acute variceal bleeding, and 60% are likely to rebleed within a year, thus endangering their lives and degrading their quality of life[1-3]. Therefore, the early identification of cirrhotic patients at risk of EGVB is essential.

Endoscopy is the gold standard for detecting patients with EGVB, which is recommended by guidelines for diagnosing and screening EGV as well as for assessing bleeding risk[4]. However, some patients refuse upper gastrointestinal endoscopy due to its invasiveness and poor tolerance. Furthermore, repeated examinations may reduce long-term compliance and thereby confound clinical observation. Moreover, endoscopy has the potential to provoke EGVB in low-risk patients, and carries the attendant risks of anesthesia. Consequently, regular follow-up through endoscopy is difficult.

The Baveno VII consensus workshop recommended that patients with compensated cirrhosis whose liver stiffness and platelet counts meet cut-off points may be spared endoscopic screening[3]. However, because the Baveno criteria have a low specificity for ruling out high-risk varices, some patients still require a subsequent endoscopy[5]. Ultrasound elastography is impeded by ascites, obesity, bowel gas, and other clinical issues. The above reasons limit the application of the Baveno criteria in clinical practice. Measurement of the hepatic venous pressure gradient serves as the gold standard for the diagnosis of portal hypertension and to assess treatment response, which is an effective tool for predicting the risk of bleeding at the EGV[3]. However, its measurement entails an invasive procedure that requires specialized operators and equipment, as well as high economic costs that limit its availability in clinical practice.

Conversely, the widespread use of computed tomography (CT) in cirrhotic patients facilitates the diagnosis and evaluation of complications. Typical CT manifestations of cirrhosis include disproportionate sizes of hepatic lobes, marked widening of hepatic fissures, wavy patterns of hepatic edges, visible gallbladder displacement, and heterogeneous hepatic parenchymal density[6]. In addition, CT images can visualize cirrhosis-related complications such as portal vein widening, portal hypertension, collateral circulation, and splenomegaly[7]. All of these manifestations can facilitate the

diagnosis of cirrhosis. Nonetheless, the utility of CT-based screening depends highly on the experience and subjective judgement of the radiologist.

Recent studies on the noninvasive assessment and prediction of EGV have made progress. Radiomics is an emerging image analysis technology that focuses on extracting high-throughput and quantitative features from medical images, using data mining algorithms to detect associations between radiographic features and diseases, and to then develop corresponding models for each feature[8]. It is used primarily for tumor diagnosis, efficacy evaluation, and prognosis[9]. Only a few studies have utilized it to assess non-neoplastic liver diseases and portal hypertension[10-14]. The CHESS team from China established the first model for predicting clinically significant portal hypertension based on radiomics features of liver and spleen, and demonstrated good diagnostic performance (area under the receiver operating characteristic curve (AUC) = 0.894)[11]. Additionally, Lin *et al*[15] evaluated the safety and efficacy of predicting high-risk EGV by combining esophageal and gastric radiomics features. By extracting CT features from hepatic, splenic, and lower esophageal regions of interest (ROIs), Liu *et al*[12] combined radiomics signature with clinical indicators to establish a prediction model to identify the likelihood esophageal variceal bleeding. Yang *et al*[14] integrated radiomics from the liver region with clinical variables to estimate the bleeding risk of EGV in cirrhosis related to hepatitis B.

However, previous radiomics models have not explored the risk of EGVB in patients with cirrhosis of varied etiologies. Furthermore, their performance has not been compared to existing noninvasive models. The establishment of a noninvasive prediction model may reduce the frequency of endoscopic examinations in patients without EGVB, while patients at risk of EGVB may receive more timely diagnosis and treatment, which is of great significance for guidance of follow-up treatment and review. Therefore, our study sought to develop a noninvasive predictive model that combines radiomics features of the liver and spleen as well as clinical indicators for predicting the risk of EGVB in patients with cirrhosis, and to evaluate its clinical utility.

MATERIALS AND METHODS

This was a retrospective study conducted at a single center, with an informed consent waiver granted by the Institutional Review Board.

Patients

Patients diagnosed with liver cirrhosis and EGV between September 2017 and December 2021 were included in our study by retrospective review. The following were the criteria for inclusion: (1) Diagnosis of cirrhosis through histopathologic examination or a combination of clinical, laboratory, and radiologic findings; (2) Completion of a triple-phase enhanced CT scan within one week prior to endoscopy; and (3) All patients diagnosed with EGV through endoscopy. Exclusion criteria were: (1) Previous endoscopic therapy, trans jugular intrahepatic portosystemic shunt, splenectomy, splenic artery embolization, balloon occlusion, retrograde transvenous occlusion, or liver transplantation; (2) Patients with liver neoplasms; and (3) Incomplete clinical or imaging data.

As a random assignment in a 7:3 ratio, patients were divided into training and validation cohorts. Finally, there were 149 patients included in the training set, as well as 62 in the validation one. A flowchart of our study is shown in Figure 1.

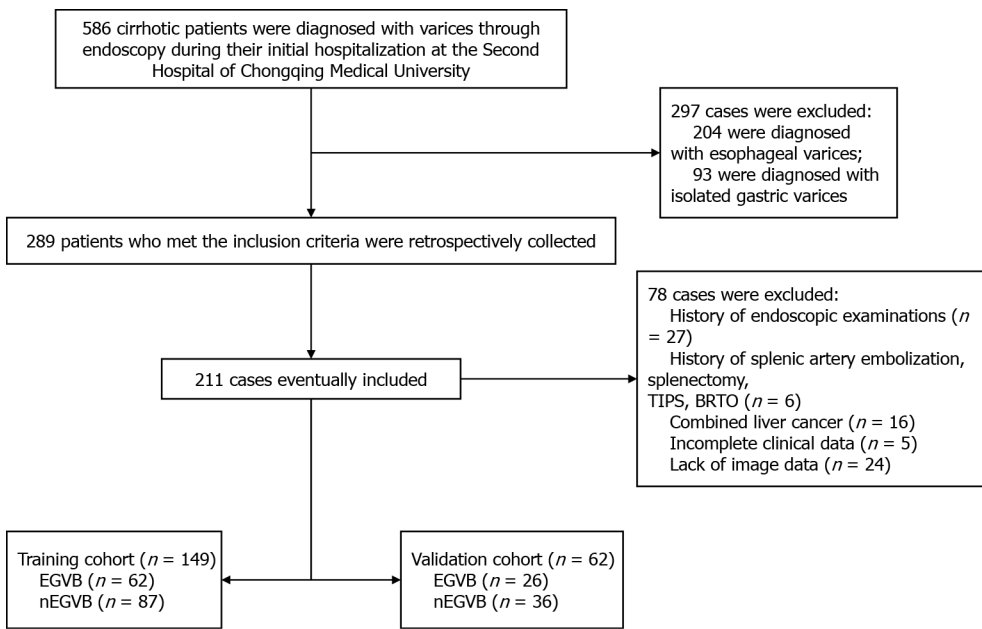
Endoscopy

Endoscopies were performed by experienced gastroenterologists. The diagnosis of EGVB-positive was based on one or more of the following signs: (1) Bleeding or exudation of the variceal region; (2) Fresh blood, with the exclusion of non-variceal hemorrhage; and (3) Signs of recent variceal bleeding (stain), such as a white thrombus or an overlying blood clot [4,16]. Ulcers, portal hypertensive gastropathy, and other non-variceal factors may also lead to upper gastrointestinal bleeding. When patients had a recent history of bleeding and endoscopy failed to find evidence of variceal hemorrhage, we considered other etiologies of bleeding such as portal hypertensive gastropathy and ulcers.

CT Scan

CT examinations were performed using a Siemens SOMATOM Force dual-source CT scanner (Siemens Healthcare). Patients were instructed to fast for more than four hours without consuming any solid food or liquids. They were allowed to drink up to 800 mL of water before scanning. Iohexol (350 mg/mL) was injected under high pressure into the cubital vein at a dose of 1.5 mL/kg and at a flow rate of 4.5 mL/s, followed by flushing with 30 mL of a saline solution. Siemens CT used contrast agent concentration tracking technology to obtain standard three-phase images of the abdominal aorta after setting a threshold of 100HU and triggering delays of 10 s, 20 s, and 15 s. Scan parameters were: tube voltage, 120 kV or 70 kV; tube current, 148 mAs; slice thickness, 1 mm; slice interval, 0 mm; and pitch ratio, 0.6. Feature extraction was performed on all images and exported in Digital Imaging and Communications in Medicine format.

Measurements of related parameters from CT images[17] were: (1) Portal vein thrombosis: endovascular filling defect of the portal vein; (2) Splenorenal/gastrorenal shunts: tortuous and thick vessels between the lesser curvature of the stomach, the splenic hilum, and left renal hilus, which may dilate and communicate with the left renal vein; (3) Upper and lower splenic diameters: The vertical distance from the upper to the lower margin of the spleen, *i.e.*, the lower pole window minus the upper pole window of the spleen; (4) Spleen diameter: The longest diameter of the spleen at the central level of the splenic hilum (antero-posterior straight line); and (5) Spleen thickness: The shortest diameter from the inner margin to the outer margin of the spleen at the central level of the splenic hilum.



DOI: 10.3748/wjg.v29.i6.1076 Copyright ©The Author(s) 2023.

Figure 1 Flowchart of inclusion and exclusion procedures for this study. TIPS: Transjugular intrahepatic portosystemic shunt; BRTO: Balloon occluded retrograde transvenous obliteration; EGVB: Esophagogastric variceal bleeding; nEGVB: Without the occurrence of esophagogastric variceal bleeding.

CT image preprocessing and ROI segmentation

After retrieving CT images from all patients, the radiologist used the 3Dslicer (V4.13.0, <https://www.slicer.org/>) to delineate ROI in the portal venous phase. ROIs of the liver and spleen were set at the levels of the hepatic and splenic hilae, respectively (Figure 2A), excluding the large blood vessels. The radiologist was blinded to the endoscopic results.

Feature extraction and selection in radiomics

Before the extraction of radiomic features, images were normalized by Gaussian filtering, wavelet bandpass filtering, and isotropic resampling. Based on ROIs, we could extract radiomics features through the Pyradiomics-based extension package Radiomics of 3Dslicer. There were 1130 radiomic features extracted for each ROI, totaling 2260 per patient.

To analyze inter- and intra-observer reliability, 30 cases were selected randomly from the total sample. After two months, two radiologists experienced in abdominal CT interpretation repeated segmentation and feature extraction for these cases. Reliability was assessed by the intraclass correlation coefficient (ICC), and was considered strongly reproducible and dependable when ICC values exceeded 0.75. Features above the ICC threshold of 0.75 were included in subsequent studies. To reduce the overfitting caused by a great number of redundant features, an independent sample t-test was applied to features and classification labels to screen out highly correlated features. Next, the least absolute shrinkage and selection operator (LASSO) regression was conducted to obtain dimensionality reduction, retain the most relevant features, and construct radiomic features from non-zero coefficient features within one standard deviation of the optimal penalty parameter lambda. A radiomics signature (RadScore) was calculated and constructed for each patient through a linear combination of selected features weighted by their respective LASSO coefficients.

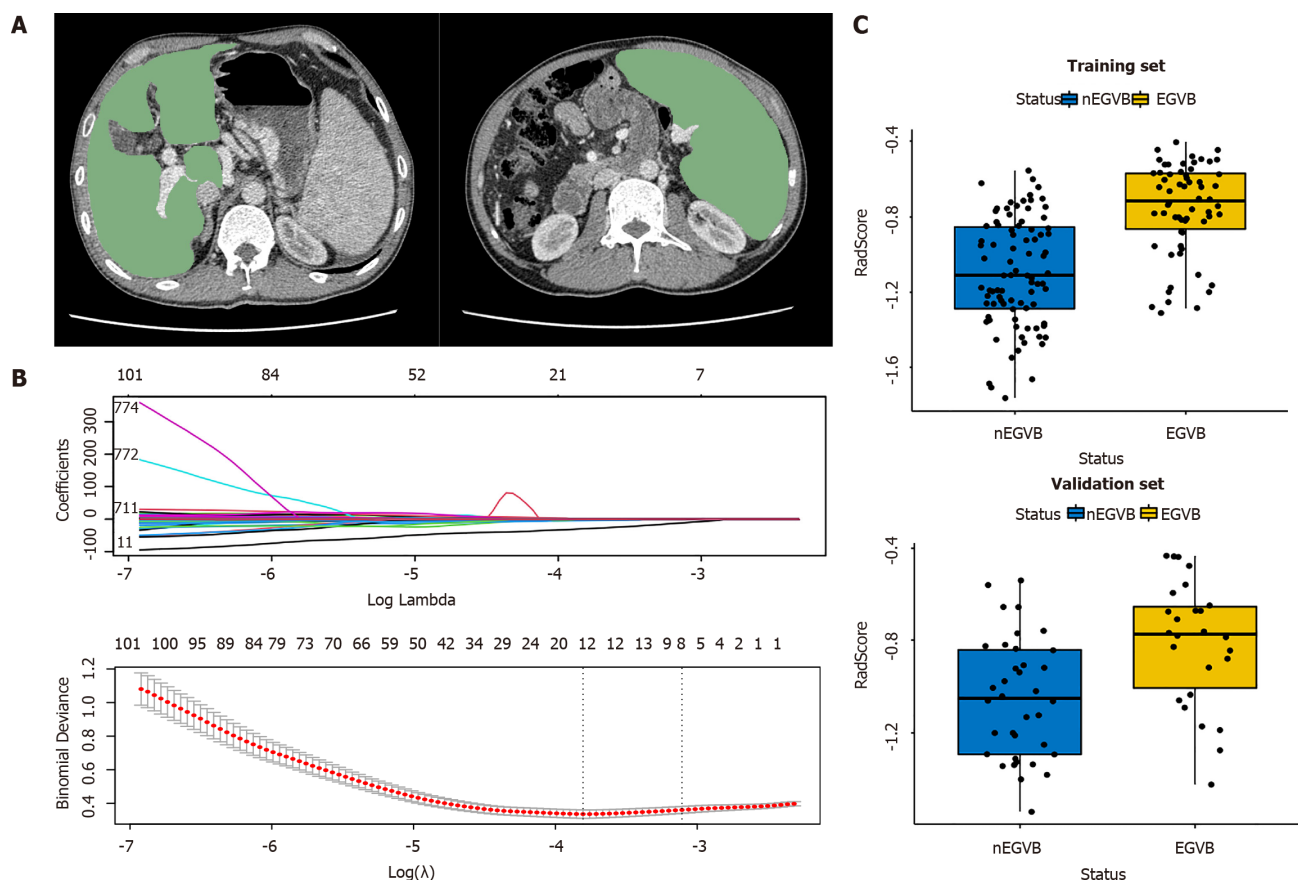
Statistical analysis

Quantitative data from normal distribution are represented by X (standard deviation), from non-normal distribution by M (P25-P75), and count data by percentage. Both univariate logistic and multiple logistic regressions with backward stepwise selection were used for the selection of independent risk factors for clinical variables. For the training and validation cohorts, we calculated the AUC the receiver operating characteristic curves to evaluate the predictive accuracy of clinical-radiomics models. Furthermore, the clinical-radiomics nomogram was subjected to decision curve and clinical impact curve analyses to determine its clinical utility and net benefit. There were two statistical analysis software programs carried out for this study: R (version 4.1.3) and Python (version 3.9.7). Statistical tests were all two-way, and it was considered statistically significant when the P -values were less than 0.05.

RESULTS

Patient characteristics

In our study, there were a total of 211 patients diagnosed with cirrhosis and EGVB (131 men and 80 women), 123 of whom were identified as EGVB-negative (nEGVB) and 88 were EGVB-positive. Thirteen were diagnosed with cirrhosis by histological examination, and the remaining 198 patients were diagnosed with cirrhosis by a combination of history,



DOI: 10.3748/wjg.v29.i6.1076 Copyright ©The Author(s) 2023.

Figure 2 Workflow of the radiomics analysis. A: The liver and spleen regions of interest were defined at the level of the hepatic hilum and the splenic hilum, respectively; B: The least absolute shrinkage and selection operator regression analysis for dimension reduction of radiomics features, and the optimal model parameter λ was selected by 10-fold cross-validation; C: The boxplots of radiomics signatures (RadScore) in the training and validation groups display notable differences respectively. EGVB: Esophagogastric variceal bleeding; nEGVB: Without the occurrence of esophagogastric variceal bleeding.

clinical manifestations, laboratory findings, and CT examination. Of these, some were hospitalized for acute decompensation events such as bleeding, ascites, and hepatic encephalopathy in a short-term period. Hemorrhage occurred primarily in the EGVB-positive group, while ascites and hepatic encephalopathy were present in both EGVB-positive and -negative groups.

From electronic medical record systems, we obtained the complete demographic and clinical data about patients. Table 1 summarizes the baseline characteristics of patients.

Radiomics Feature Selection and Radiomics Signature Construction

Based on an independent sample t-test and LASSO regression, eight radiomics features were selected, five from the liver and three from the spleen (Figure 2B). Through weighting the LASSO coefficients of the selected features, we established a radiomics signature (RadScore). The specific formula of RadScore is shown in the supplementary material. The boxplots in the training and validation cohorts indicated that RadScores differed remarkably ($P < 0.001$) (Figure 2C).

Model Construction and Evaluation

Univariate analysis screened out clinical features that were significantly related to EGVB ($P < 0.05$). To minimize the effects of multicollinearity, we performed a multivariate backward stepwise regression to confirm portal vein thrombosis, aspartate aminotransferase (AST), albumin, fibrinogen, and spleen thickness as independent risk factors for EGVB ($P < 0.05$) (Table 2). The variance inflation factor was less than 4.

By combining independent clinical predictors with RadScore, a clinical-radiomics nomogram was established by generalized linear regression (Figure 3). The calibration curve performed well in both training and validation groups, with Hosmer-Lemeshow test results of $P = 0.775$ (Figure 4A) and $P = 0.391$ (Figure 4B) respectively, indicating that the nomogram's predictive power and the actual risk of developing EGVB did not differ significantly. As shown in the training set (Figure 5A), the clinical-radiomics nomogram demonstrated excellent predictive performance with an AUC of 0.925 (95%CI: 0.883-0.967) and 0.912 (95%CI: 0.845-0.98) as shown in the validation set (Figure 5B). Furthermore, compared with other noninvasive methods such as APRI and FIB-4 reported in studies previously, our clinical-radiomics nomogram exhibited the highest diagnostic accuracy, with Delong test of less than 0.05. Decision curve analysis showed that the clinical-radiomics nomogram had a high clinical applicability that exceeded those of existing noninvasive serum-based predictive models such as APRI and FIB-4 in both the training (Figure 6A) and validation (Figure 6B) sets.

Table 1 Baseline characteristics of patients in the training and validation cohort

Characteristics	Train cohort		Validation cohort	
	nEGVB (n = 87)	EGVB (n = 62)	nEGVB (n = 36)	EGVB (n = 26)
Sex (Male)	54 (62.1%)	40 (64.5%)	21 (58.3%)	16 (61.5%)
Age(yr)	55.0 (36.0, 83.0)	53.0 (15.0, 79.0)	52.0 (10.8)	52.9 (12.5)
Etiology				
HBV	58 (66.7%)	38 (61.3%)	19 (52.8%)	16 (61.5%)
HCV	5 (5.7%)	6 (9.7%)	3 (8.3%)	1 (3.8%)
Alcohol	4 (4.6%)	7 (11.3%)	3 (8.3%)	3 (11.5%)
Others	20 (23.0%)	11 (17.7%)	11 (30.6%)	6 (23.1%)
Portal vein thrombosis	5 (5.7%)	21 (33.9%)	1 (2.8%)	8 (30.8%)
Shunt	21 (24.1%)	21 (33.9%)	14 (38.9%)	9 (34.6%)
HE	1 (1.1%)	6 (9.7%)	0 (0%)	2 (7.7%)
Ascites				
0	40 (46.0%)	9 (14.5%)	13 (36.1%)	6 (23.1%)
1	31 (35.6%)	45 (72.6%)	22 (61.1%)	17 (65.4%)
2	5 (5.7%)	6 (9.7%)	1 (2.8%)	2 (7.7%)
3	11 (12.6%)	2 (3.2%)	0 (0%)	1 (3.8%)
Child-Pugh score				
A	33 (37.9%)	16 (25.8%)	15 (41.7%)	9 (34.6%)
B	47 (54.0%)	38 (61.3%)	17 (47.2%)	14 (53.8%)
C	7 (8.0%)	8 (12.9%)	4 (11.1%)	3 (11.5%)
PLT (10 ⁹ /L)	60.0 (17.0, 186)	72.5 (21.0, 245)	53.0 (16.0, 192)	60.0 (26.0, 208)
PT (s)	15.6 (12.4, 24.9)	16.1 (11.7, 26.8)	16.1 (3.30, 22.3)	17.1 (14.1, 31.6)
APTT (s)	39.7 (29.5, 57.3)	38.9 (30.1, 53.1)	41.5 (34.2, 51.0)	38.2 (30.7, 63.6)
INR	1.22 (0.92, 2.18)	1.28 (0.85, 2.51)	1.29 (0.98, 1.95)	1.39 (1.10, 3.00)
Fib (g/L)	2.19 (0.75, 6.09)	1.78 (0.60, 5.78)	2.11 (0.489)	1.80 (0.628)
Albumin (g/L)	34.1 (18.4, 46.3)	32.3 (21.3, 45.9)	33.6 (6.36)	30.8 (5.28)
Tbil (μmol/L)	21.9 (2.20, 366)	16.9 (3.60, 93.0)	23.5 (6.40, 414)	18.5 (7.00, 76.1)
DBil (μmol /L)	9.80 (0.90, 276)	8.05 (1.90, 65.9)	10.8 (2.30, 306)	8.70 (2.70, 38.5)
Prealbumin (mg/L)	90.0 (12.0, 220)	97.5 (18.0, 246)	85.0 (9.00, 268)	83.5 (18.0, 221)
ALT (U/L)	36.0 (7.00, 345)	23.0 (10.0, 85.0)	41.0 (14.0, 337)	22.5 (10.0, 107)
AST (U/L)	47.0 (15.0, 330)	29.5 (11.0, 92.0)	48.0 (23.0, 319)	25.5 (17.0, 121)
SL (mm)	130 (89.1, 206)	142 (78.8, 200)	143 (98.7, 199)	139 (109, 205)
SD (mm)	144 (82.0, 235)	157 (68.8, 299)	152 (86.0, 239)	174 (109, 222)
ST (mm)	45.1 (9.22)	52.5 (11.1)	48.3 (30.5, 84.5)	55.2 (29.9, 64.8)

EGVB: Esophagogastric variceal bleeding; nEGVB: Without the occurrence of esophagogastric variceal bleeding; HE: Hepatic encephalopathy; PLT: Platelet. PT: Prothrombin time; APTT: Activated partial thromboplastin time; INR: International prothrombin ratio; Fib: Fibrinogen; Tbil: Total bilirubin; DBil: Direct bilirubin; ALT: Alanine aminotransferase; AST: Aspartate aminotransferase; SL: Spleen upper and lower diameter; SD: Spleen diameter; ST: Spleen thickness.

Table 2 Univariate and multivariate analysis of factors associated with the presence of esophagogastric variceal bleeding in cirrhotic patients

Variables	Univariate logistic regression		Multivariate logistic regression	
	OR (95%CI)	P value	OR (95%CI)	P value
Age	0.98 (0.949-1.01)	0.183	-	-
Albumin	0.925 (0.866-0.984)	0.01	0.84 (0.753-0.926)	< 0.001
ALT	0.962 (0.941-0.984)	0.001	-	-
APTT	0.945 (0.876-1.01)	0.107	-	-
AST	0.962 (0.942-0.981)	< 0.001	0.941 (0.913-0.97)	< 0.001
DBil	0.968 (0.926-1.01)	0.122	-	-
Etiology	1.832 (-0.094-3.76)	0.661	-	-
Fib	0.46 (-0.061-0.982)	0.004	0.385 (-0.17-0.939)	0.001
INR	5.613 (4.26-6.97)	0.013	-	-
PLT	1.007 (0.998-1.02)	0.11	-	-
Portal vein thrombosis	8.4 (7.36-9.44)	< 0.001	9.15 (7.78-10.5)	0.002
HE	9.214 (7.07-11.4)	0.042	-	-
Child-Pugh score	1.668 (1.07-2.26)	1.365	-	-
Ascites	6.452 (6.87-6.03)	0.853	-	-
Prealbumin	1.002 (0.995-1.01)	0.525	-	-
PT	1.188 (1.05-1.33)	0.015	-	-
SD	1.01 (1-1.02)	0.016	-	-
Sex	0.9 (0.223-1.58)	0.76	-	-
Shunt	1.61 (0.89-2.33)	0.195	-	-
SL	1.012 (0.999-1.02)	0.075	-	-
ST	1.078 (1.04-1.12)	< 0.001	1.056 (1.01-1.1)	0.025
Tbil	0.979 (0.955-1)	0.08	-	-

HE: Hepatic encephalopathy; PLT: Platelet; PT: Prothrombin time; APTT: Activated partial thromboplastin time; INR: International prothrombin ratio; Fib: Fibrinogen; Tbil: Total bilirubin; DBil: Direct bilirubin; ALT: Alanine aminotransferase; AST: Aspartate aminotransferase; SL: Spleen upper and lower diameter; SD: Spleen diameter; ST: Spleen thickness.

Moreover, the clinical impact curve of the nomogram was constructed based on 1,000 simulated samples, which revealed that the nomogram yielded an event probability that corresponded closely to actual high risk when the risk threshold was between 0.4 and 0.8, and consistently when it exceeded 0.8 (Figure 7).

DISCUSSION

With a high mortality and morbidity rate, EGVB is among the most serious complications related to decompensated cirrhosis[1]. A routine endoscopic examination is recommended as a diagnostic method for assessing the grade and bleeding risk of EGV[4]. However, the bleeding risk of invasive procedures, contraindications to anesthesia, and unnecessarily excessive endoscopic examinations limit its clinical application and, to some extent, lead patients to forego their follow-ups. In recent years, there has been an increasing demand for noninvasive methods to estimate the risk of EGVB in cirrhotic patients. Noninvasive diagnostic methods such as ultrasonography, magnetic resonance imaging, and CT have both advantages and disadvantages[18-20], and there are no standardized noninvasive models for EGVB that can be used widely in clinical practice.

Radiomics is an emerging diagnostic tool that has the ability to extract numerous image features noninvasively and describe modules for quantitatively evaluating gray scales and pixel distribution in medical images, which are undetectable by the naked eye[21]. It has yielded satisfactory results, and has become increasingly popular in diagnosis, assessment of treatment response, and prognosis in recent years[8]. It can comprehensively describe ROIs from the perspectives of morphology, histogram, texture, and higher-order features such as texture features extracted through

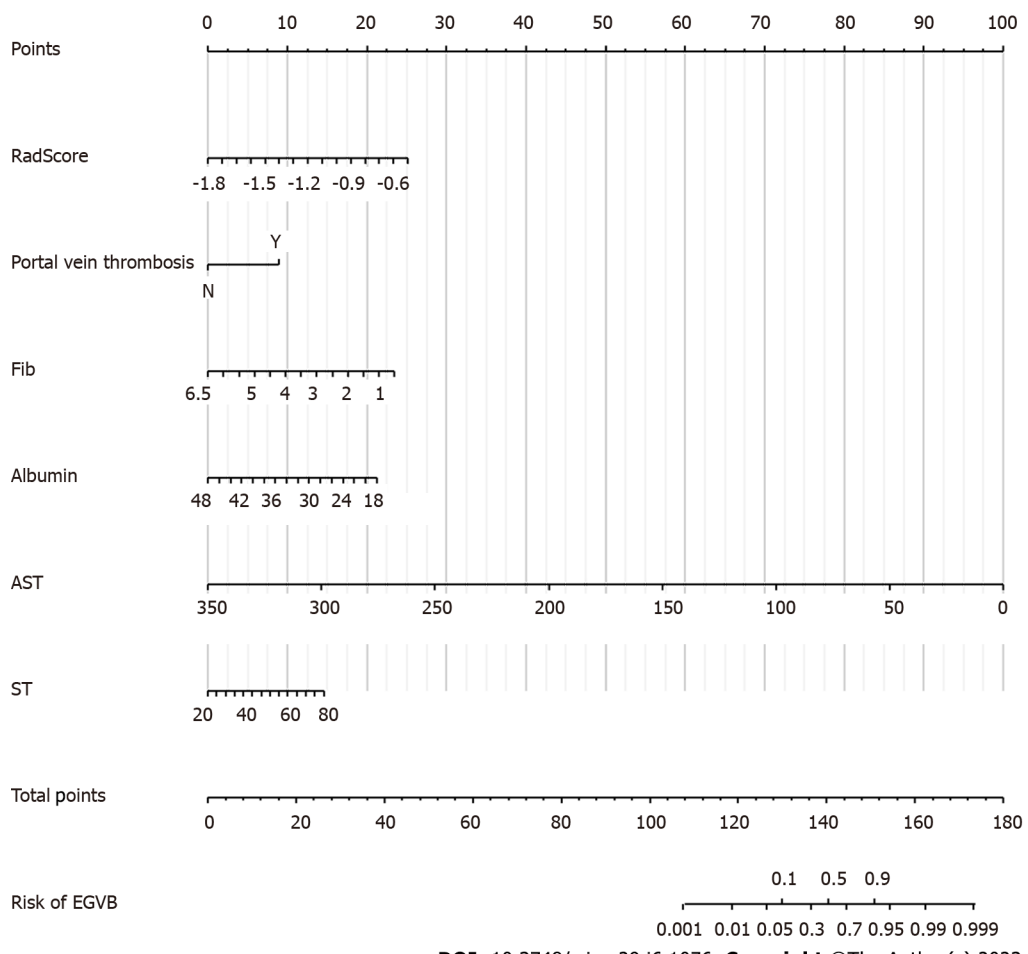


Figure 3 The construction of a clinical-radiomics prediction model for esophagogastric variceal bleeding. The clinical-radiomics nomogram for predicting bleeding risk. The scores of the different variables in the nomogram were summed to obtain the total score, and a line was drawn from the axis of the total score to the bottom line to determine the probability of bleeding risk. Fib: Fibrinogen; AST: Aspartate aminotransferase; ST: Spleen thickness; EGVB: Esophagogastric variceal bleeding.

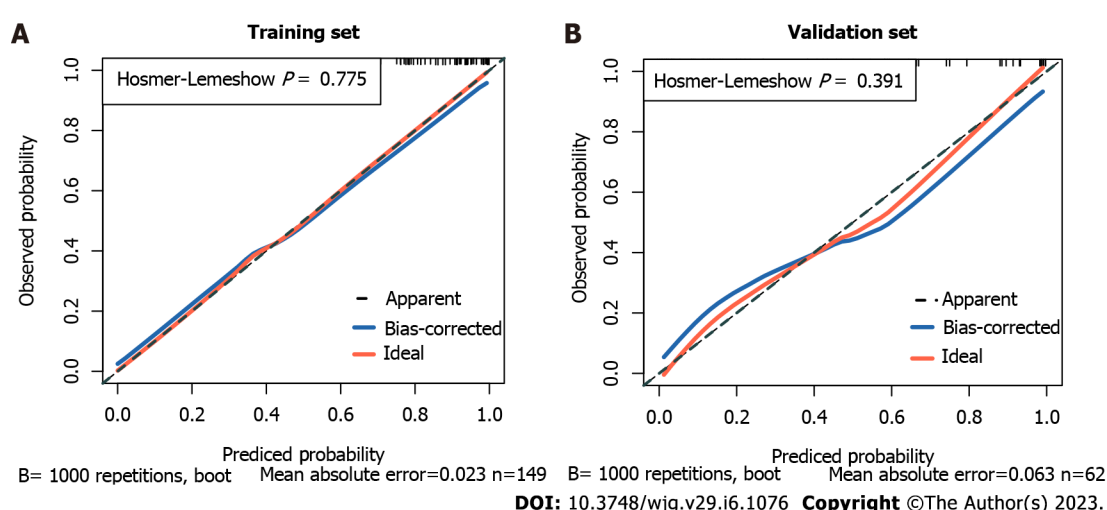


Figure 4 The calibration curves of the nomogram. A: The calibration curve of the nomogram shows a good fit in the training cohort ($P = 0.775$); B: The calibration curve of the nomogram shows a good fit in the validation cohort ($P = 0.391$).

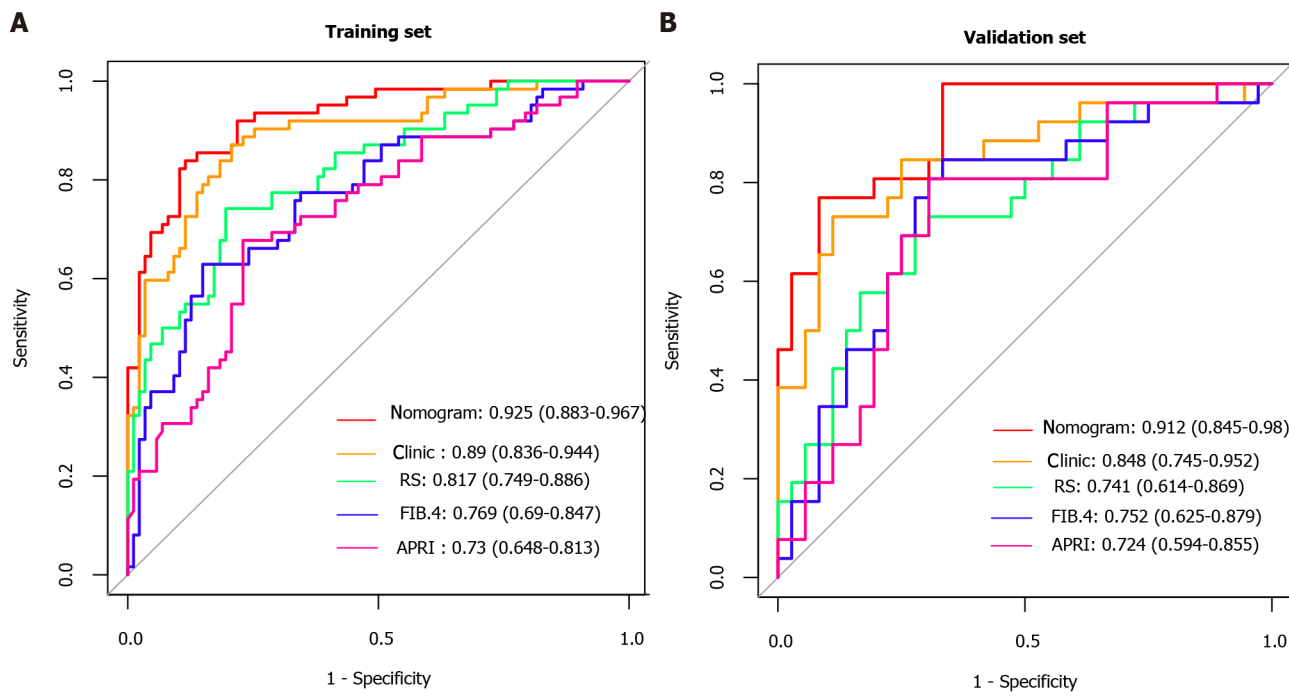


Figure 5 The receiver operating characteristic curves in the study. A: The receiver operating characteristic curves (ROC) in the training cohort; B: The ROCs in the validation cohort. Clinic: The model based on clinical individual indicator; RS: Radiomics Signature (RadScore); APRI: Ratio of aspartate aminotransferase to platelets; FIB.4: Fibrosis-4 scores.

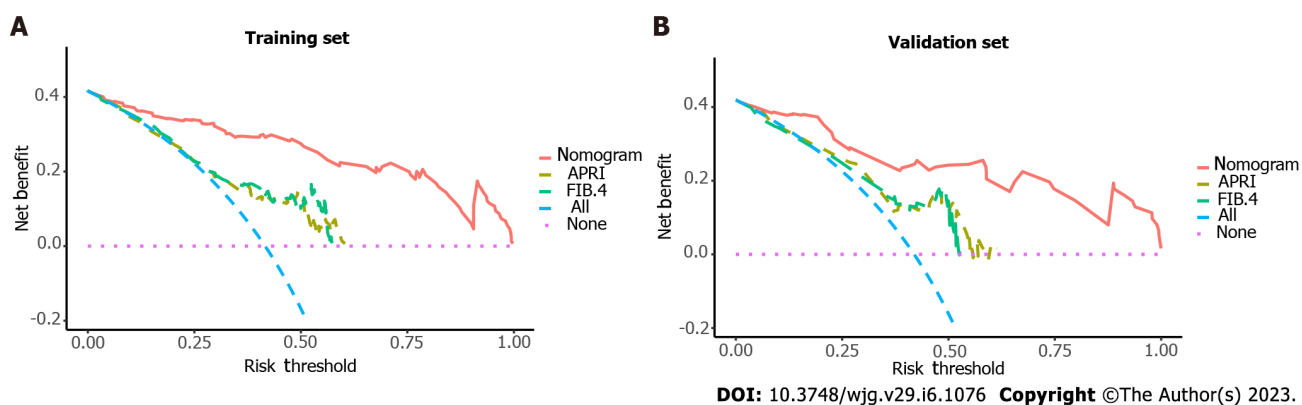
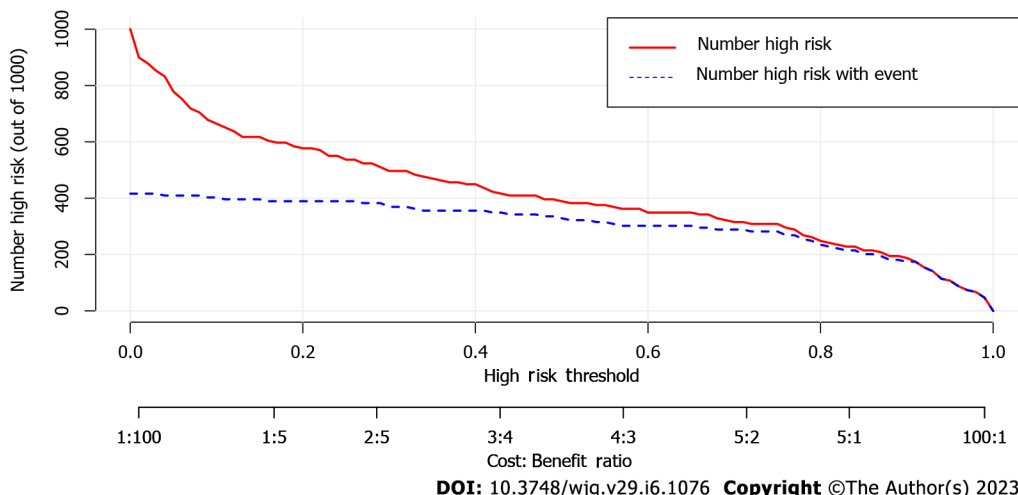


Figure 6 The clinical decision curves for bleeding prediction. A: The training cohort; B: The validation cohort. A threshold probability is the point at which the expected benefits of a treatment equal those of not receiving treatment. As shown by the different lines in the diagram, red indicates the clinical-radiomics nomogram, green indicates Fibrosis-4 scores (FIB.4), yellow indicates Ratio of aspartate aminotransferase to platelets (APRI), pink indicates the hypothesis of patients without esophagogastric variceal bleeding (EGVB), and blue indicates that all patients developed EGVB. They indicate that the clinical-radiomics nomogram is superior to the non-invasive serum predictive model's APRI and FIB.4 in terms of clinical utility. APRI: Ratio of aspartate aminotransferase to platelets; FIB.4: Fibrosis-4 scores.

Gaussian, wavelet, and other filtration methods[22].

We constructed a RadScore based on five liver features and three spleen features. Among them, 5 texture and 3 histogram features were extracted, 7 of which were higher-order filtered features. Small Area Low Gray Level Emphasis, Size Zone Non Uniformity Normalized, Short Run High Gray Level Emphasis, Cluster Shade, and Imc1 are texture features[23]. As crucial components of radiomics features, they combine pixels and shapes, and thereby describe the spatial relationships of adjacent pixels. Kurtosis, Skewness and Maximum are histogram features that emphasize the distribution pattern of gray-level pixel values within ROIs[23]. RadScore can accurately predict EGVB risk as evidenced AUCs of both the training and validation sets, and performed better in the validation group in comparison to Yang *et al* [14]'s previous study that only included liver ROIs.

There is no single radiomics model which is capable of fully reflecting the characteristics of the disease. Consequently, multiparametric, multi-omics, and multivariate models have generated increasing interest. By incorporating readily available independent clinical predictors and RadScore, diagnostic performance has been further enhanced, with an AUC of 0.925 (95%CI: 0.883-0.967) and 0.912 (95%CI: 0.845-0.98) in the training and validation sets, respectively. Meanwhile,



DOI: 10.3748/wjg.v29.i6.1076 Copyright ©The Author(s) 2023.

Figure 7 Clinical impact curve of the nomogram for 1,000 simulated samples. The blue dashed line is the actual high-risk number, and the red line is the high-risk number based on the nomogram. The nomogram predicted a probability of the event that corresponded closely to its actual high risk when the risk threshold was between 0.4 and 0.8, and consistently when it exceeded 0.8.

our combined model performed better in predicting EGV than other noninvasive methods (such as APRI and FIB-4) that have been fully validated in previous studies. Decision curve analysis showed that the clinical-radiomics nomogram can yield a good net benefit in clinical applications. The reduced AUCs of all models in the validation cohort are readily apparent, and may have been caused by the small sample size. In addition, the EGV group included 29 patients with variceal bleeding at the esophagogastric junction and 27 at the gastric fundus. To some extent, our model could predict the overall risk of variceal bleeding in the esophagogastric junction and gastric fundus. However, no radiomics-related studies have specifically addressed the risk of variceal bleeding at these two anatomic sites. Prospective exploration and analysis in follow-up studies are necessary.

Cirrhosis features fibrosis and regenerative hepatic nodules that compress sinusoids, resulting in sinusoidal narrowing that promotes vascular collateralization[1]. Furthermore, portal hypertension predisposes to branched splenic vein obstruction, leading to congestive splenomegaly and hypersplenism. Numerous studies have confirmed associations between liver, spleen, and portal hypertension[18,24]. In earlier studies of radiomics models for predicting variceal bleeding in cirrhosis, Liu's research only examined esophageal variceal bleeding[12], and Yang *et al*'s study only included liver ROIs[14]. In contrast to previous reports, we included patients with cirrhosis of multiple etiologies and extracted hepatic and splenic features simultaneously. Additionally, our combined model showed a better performance in comparison with other multivariate ones.

Our study found that portal vein thrombosis, fibrinogen, AST, albumin, and spleen thickness were independent risk factors for EGV in patients with cirrhosis. According to previous studies, portal vein thrombosis is one of the risk factors for EGV in liver cirrhosis, which may be related to the increased portal pressure to some extent[25,26]. Impaired hepatic synthetic capacity disturbs procoagulant (*e.g.*, fibrinogen) and anticoagulant balance, resulting in coagulopathies. The decrease of fibrinogen may result in an inefficient removal of activated coagulation factors and ultimately increase the risk of bleeding. AST is a functional hepatic enzyme that can indirectly reflect hepatocellular injury. Albumin and spleen thickness are significantly correlated with the presence of EGV, and were considered as risk factors in previous research [27-29]. In contrast to several previous studies, we found that platelet count was not an independent clinical predictor and may be related to its predisposing factors such as hypersplenism, antibody-mediated destruction (primarily during viral hepatitis), reductions in thrombopoietin, and bone marrow toxicity caused by hepatitis viruses and alcohol. The Child Pugh score can reflect hepatic functional reserve, often as a prognostic indicator in patients with cirrhosis. Most of the patients in our retrospective study had splenomegaly and hypersplenism, and Child Pugh scores were predominantly grade B in both the EGV and nEGV groups. Child Pugh scores, platelet counts, and total bilirubin levels were similar between the two groups ($P > 0.05$). Similar results were also shown previously[30,31].

Several limitations have been identified in our study. Firstly, this is a small-scale single-center retrospective study. Large, multicenter and prospective studies will be required to verify the model's feasibility in the future. Moreover, there is no relevant study to explore the performance of models in predicting the risk of bleeding in patients with different Child Pugh class. Our study has demonstrated that there was no significant difference in the Child Pugh scores between the EGV and nEGV group, and the prediction model performed well in assessing the risk of bleeding on the whole. Exploring the diagnostic performance of the model for bleeding risk in patients with different Child Pugh class can facilitate further refining the risk stratification of patients and achieve precision medicine, which should be investigated in subsequent research. Secondly, elastography can predict portal hypertension and EGV to some extent by measuring liver and spleen stiffness. Lin *et al*[15] compared a radiomics nomogram with liver stiffness measurement through transient elastography in a subgroup of 42 patients, showing the nomogram was superior in predicting high-risk EGV. However, comparisons of elastography with radiomics models to predict variceal bleeding are lacking. In our retrospective study, most patients did not undergo elastography. We failed to retrieve the relevant data, which we see as

a shortcoming of our study. The comparison of elastography with radiomics models is crucial, and should be conducted in the later studies. Thirdly, more in-depth investigations of multi-image and multi-omics (such as metabolomics, genomics, etc.) were not conducted. For subsequent studies of EGVB, multi-modal and multi-omics models, deep learning, and other methods should be fully employed.

CONCLUSION

We established a multivariate prediction model based on CT radiomics features and clinical characteristics, which demonstrated good performance for predicting EGVB in cirrhotic patients. Aided by clinical-radiomics nomogram, clinicians can base therapeutic decisions on fewer invasive procedures while personalizing follow-up treatment.

ARTICLE HIGHLIGHTS

Research background

Esophagogastric variceal bleeding (EGVB) is a fatal complication of liver cirrhosis, which requires aggressive intervention. Prediction of bleeding risk in cirrhotic patients with esophagogastric varices (EGV) is beneficial to individualized treatment and improve prognosis. Radiomics, an emerging field, has a good performance in disease diagnosis and efficacy evaluation.

Research motivation

Currently, there is still a lack of noninvasive models that can be widely used in clinical practice to predict the risk of bleeding in liver cirrhosis.

Research objectives

Our study aimed to develop and validate a novel predictive model based on radiomics extracted from contrast-enhanced computed tomography (CT) and clinical indicators to noninvasively assess the risk of bleeding in cirrhotic patients with EGV.

Research methods

211 patients were divided into training and validation cohorts in a 7:3 ratio. Radiomics features were extracted from the portal venous phase CT images, and a radiomics signature (RadScore) was constructed through further feature dimension reduction and screening. The univariate and multivariate logistic regression analyses were preformed to select independent clinical predictors. Finally, a combined model was established based on RadScore and clinical variables. The receiver operating characteristic curves, calibration curves, clinical decision curves and clinical impact curves were applied to evaluate the performance of the model.

Research results

The RadScore was constructed from 8 radiomics features. Albumin, fibrinogen, portal vein thrombosis, aspartate aminotransferase, and spleen thickness were selected as independent predictors. The nomogram, combining RadScore and clinical variables, demonstrated good diagnostic performance in both the training and validation cohorts (area under the receiver operating characteristic curve (AUC) = 0.925 and 0.912, respectively), which outperformed existing non-invasive models such as ratio of aspartate aminotransferase to platelets and Fibrosis-4 scores (Delong test < 0.05).

Research conclusions

The combined model based on radiomics features and clinical indicators shows good predictive accuracy and can contribute to noninvasively assessing the risk of EGVB in patients with cirrhosis.

Research perspectives

Radiomics has shown good diagnostic performance in the assessment of portal hypertension and the identification of high-risk esophageal varices. Our study demonstrated that the model combined clinical variables and radiomics features has the potential utility for non-invasive prediction of EGVB. Further large-scale, multi-center prospective studies are still required to verify its performance in the future.

FOOTNOTES

Author contributions: Luo R was responsible for designing the study, collecting data, analyzing data, and writing the paper; Gao J was responsible for designing the study and guiding important content of the article; Gan W and Xie WB were responsible for providing technical support. All authors approved the final version of the manuscript for submission for publication.

Supported by Kuanren Talents Program of The Second Affiliated Hospital of Chongqing Medical University.

Institutional review board statement: The study was reviewed and approved by the Ethics Committee of the Second Affiliated Hospital of Chongqing Medical University (No. 2022-149).

Informed consent statement: Our study was a retrospective study conducted at a single center. We used data from patients at the time they were treated in the hospital, and these data were collected and analyzed anonymously. The informed consent waiver was granted by the Institutional Review Board.

Conflict-of-interest statement: The authors declare that the research was conducted in the absence of any commercial or financial relationships.

Data sharing statement: No additional data are available.

Open-Access: This article is an open-access article that was selected by an in-house editor and fully peer-reviewed by external reviewers. It is distributed in accordance with the Creative Commons Attribution NonCommercial (CC BY-NC 4.0) license, which permits others to distribute, remix, adapt, build upon this work non-commercially, and license their derivative works on different terms, provided the original work is properly cited and the use is non-commercial. See: <https://creativecommons.org/Licenses/by-nc/4.0/>

Country/Territory of origin: China

ORCID number: Rui Luo 0000-0002-5264-396X; Jian Gao 0000-0002-7761-4444.

S-Editor: Liu GL

L-Editor: Filipodia

P-Editor: Liu GL

REFERENCES

- 1 Lesmana CRA, Raharjo M, Gani RA. Managing liver cirrhotic complications: Overview of esophageal and gastric varices. *Clin Mol Hepatol* 2020; **26**: 444-460 [PMID: 33053928 DOI: 10.3350/cmh.2020.0022]
- 2 Jakab SS, Garcia-Tsao G. Evaluation and Management of Esophageal and Gastric Varices in Patients with Cirrhosis. *Clin Liver Dis* 2020; **24**: 335-350 [PMID: 32620275 DOI: 10.1016/j.cld.2020.04.011]
- 3 de Franchis R, Bosch J, Garcia-Tsao G, Reiberger T, Ripoll C; Baveno VII Faculty. Baveno VII - Renewing consensus in portal hypertension. *J Hepatol* 2022; **76**: 959-974 [PMID: 35120736 DOI: 10.1016/j.jhep.2021.12.022]
- 4 Garcia-Tsao G, Abraldes JG, Berzigotti A, Bosch J. Portal hypertensive bleeding in cirrhosis: Risk stratification, diagnosis, and management: 2016 practice guidance by the American Association for the study of liver diseases. *Hepatology* 2017; **65**: 310-335 [PMID: 27786365 DOI: 10.1002/hep.28906]
- 5 Stafylidou M, Paschos P, Katsoulas A, Malandris K, Ioakim K, Bekiari E, Haidich AB, Akriviadis E, Tsapas A. Performance of Baveno VI and Expanded Baveno VI Criteria for Excluding High-Risk Varices in Patients With Chronic Liver Diseases: A Systematic Review and Meta-analysis. *Clin Gastroenterol Hepatol* 2019; **17**: 1744-1755.e11 [PMID: 31077823 DOI: 10.1016/j.cgh.2019.04.062]
- 6 Brancatelli G, Federle MP, Ambrosini R, Lagalla R, Carriero A, Midiri M, Vilgrain V. Cirrhosis: CT and MR imaging evaluation. *Eur J Radiol* 2007; **61**: 57-69 [PMID: 17145154 DOI: 10.1016/j.ejrad.2006.11.003]
- 7 Aubé C, Bazerbes P, Lebigot J, Cartier V, Boursier J. Liver fibrosis, cirrhosis, and cirrhosis-related nodules: Imaging diagnosis and surveillance. *Diagn Interv Imaging* 2017; **98**: 455-468 [PMID: 28461073 DOI: 10.1016/j.diii.2017.03.003]
- 8 Lambin P, Leijenaar RTH, Deist TM, Peerlings J, de Jong EEC, van Timmeren J, Sanduleanu S, Larue RTHM, Even AJG, Jochems A, van Wijk Y, Woodruff H, van Soest J, Lustberg T, Roelofs E, van Elmpt W, Dekker A, Mottaghy FM, Wildberger JE, Walsh S. Radiomics: the bridge between medical imaging and personalized medicine. *Nat Rev Clin Oncol* 2017; **14**: 749-762 [PMID: 28975929 DOI: 10.1038/nrclinonc.2017.141]
- 9 Liu Z, Wang S, Dong D, Wei J, Fang C, Zhou X, Sun K, Li L, Li B, Wang M, Tian J. The Applications of Radiomics in Precision Diagnosis and Treatment of Oncology: Opportunities and Challenges. *Theranostics* 2019; **9**: 1303-1322 [PMID: 30867832 DOI: 10.7150/thno.30309]
- 10 Meng D, Wei Y, Feng X, Kang B, Wang X, Qi J, Zhao X, Zhu Q. CT-Based Radiomics Score Can Accurately Predict Esophageal Variceal Rebleeding in Cirrhotic Patients. *Front Med (Lausanne)* 2021; **8**: 745931 [PMID: 34805214 DOI: 10.3389/fmed.2021.745931]
- 11 Liu F, Ning Z, Liu Y, Liu D, Tian J, Luo H, An W, Huang Y, Zou J, Liu C, Wang L, Liu Z, Qi R, Zuo C, Zhang Q, Wang J, Zhao D, Duan Y, Peng B, Qi X, Zhang Y, Yang Y, Hou J, Dong J, Li Z, Ding H. Development and validation of a radiomics signature for clinically significant portal hypertension in cirrhosis (CHESS1701): a prospective multicenter study. *EBioMedicine* 2018; **36**: 151-158 [PMID: 30268833 DOI: 10.1016/j.ebiom.2018.09.023]
- 12 Liu H, Sun J, Liu G, Liu X, Zhou Q, Zhou J. Establishment of a non-invasive prediction model for the risk of oesophageal variceal bleeding using radiomics based on CT. *Clin Radiol* 2022; **77**: 368-376 [PMID: 35241274 DOI: 10.1016/j.crad.2022.01.046]
- 13 Wan S, Wei Y, Zhang X, Liu X, Zhang W, He Y, Yuan F, Yao S, Yue Y, Song B. Multiparametric radiomics nomogram may be used for predicting the severity of esophageal varices in cirrhotic patients. *Ann Transl Med* 2020; **8**: 186 [PMID: 32309333 DOI: 10.21037/atm.2020.01.122]
- 14 Yang JQ, Zeng R, Cao JM, Wu CQ, Chen TW, Li R, Zhang XM, Ou J, Li HJ, Mu QW. Predicting gastro-oesophageal variceal bleeding in hepatitis B-related cirrhosis by CT radiomics signature. *Clin Radiol* 2019; **74**: 976.e1-976.e9 [PMID: 31604574 DOI: 10.1016/j.crad.2019.08.028]
- 15 Lin Y, Li L, Yu D, Liu Z, Zhang S, Wang Q, Li Y, Cheng B, Qiao J, Gao Y. A novel radiomics-platelet nomogram for the prediction of gastroesophageal varices needing treatment in cirrhotic patients. *Hepatol Int* 2021; **15**: 995-1005 [PMID: 34115257 DOI: 10.1007/s12072-021-10208-4]

- 16 de Franchis R; Baveno VI Faculty. Expanding consensus in portal hypertension: Report of the Baveno VI Consensus Workshop: Stratifying risk and individualizing care for portal hypertension. *J Hepatol* 2015; **63**: 743-752 [PMID: 26047908 DOI: 10.1016/j.jhep.2015.05.022]
- 17 Kang HK, Jeong YY, Choi JH, Choi S, Chung TW, Seo JJ, Kim JK, Yoon W, Park JG. Three-dimensional multi-detector row CT portal venography in the evaluation of portosystemic collateral vessels in liver cirrhosis. *Radiographics* 2002; **22**: 1053-1061 [PMID: 12235335 DOI: 10.1148/radiographics.22.5.g02se011053]
- 18 Liu Y, Tan HY, Zhang XG, Zhen YH, Gao F, Lu XF. Prediction of high-risk esophageal varices in patients with chronic liver disease with point and 2D shear wave elastography: a systematic review and meta-analysis. *Eur Radiol* 2022; **32**: 4616-4627 [PMID: 35166896 DOI: 10.1007/s00330-022-08601-0]
- 19 Hoffman DH, Ayoola A, Nickel D, Han F, Chandarana H, Babb J, Shanbhogue KP. MR elastography, T1 and T2 relaxometry of liver: role in noninvasive assessment of liver function and portal hypertension. *Abdom Radiol (NY)* 2020; **45**: 2680-2687 [PMID: 32274552 DOI: 10.1007/s00261-020-02432-7]
- 20 Manchec B, Pham E, Noor M, Pepe J, Feranec N, Contreras F, Ward TJ. Contrast-Enhanced CT May Identify High-Risk Esophageal Varices in Patients With Cirrhosis. *AJR Am J Roentgenol* 2020; **215**: 617-623 [PMID: 32755158 DOI: 10.2214/AJR.19.22474]
- 21 Mayerhoefer ME, Materka A, Langs G, Häggström I, Szczypiński P, Gibbs P, Cook G. Introduction to Radiomics. *J Nucl Med* 2020; **61**: 488-495 [PMID: 32060219 DOI: 10.2967/jnumed.118.222893]
- 22 Park HJ, Park B, Lee SS. Radiomics and Deep Learning: Hepatic Applications. *Korean J Radiol* 2020; **21**: 387-401 [PMID: 32193887 DOI: 10.3348/kjr.2019.0752]
- 23 Zwanenburg A, Vallières M, Abdalah MA, Aerts HJWL, Andrareczyk V, Apte A, Ashrafinia S, Bakas S, Beukinga RJ, Boellaard R, Bogowicz M, Boldrini L, Buvat I, Cook GJR, Davatzikos C, Depersinge A, Desserot MC, Dinapoli N, Dinh CV, Echegaray S, El Naqa I, Fedorov AY, Gatta R, Gillies RJ, Goh V, Götz M, Guckenberger M, Ha SM, Hatt M, Isensee F, Lambin P, Leger S, Leijenaar RTH, Lenkowicz J, Lippert F, Losnegård A, Maier-Hein KH, Morin O, Müller H, Napel S, Nioche C, Orlhac F, Pati S, Pfahler EAG, Rahimim A, Rao AUK, Scherer J, Siddique MM, Sijtsma NM, Socarras Fernandez J, Spezi E, Steenbakkers RJHM, Tanadini-Lang S, Thorwarth D, Troost EGC, Upadhyaya T, Valentini V, van Dijk LV, van Griethuysen J, van Velden FHP, Whybra P, Richter C, Löck S. The Image Biomarker Standardization Initiative: Standardized Quantitative Radiomics for High-Throughput Image-based Phenotyping. *Radiology* 2020; **295**: 328-338 [PMID: 32154773 DOI: 10.1148/radiol.2020191145]
- 24 Reiberger T. The Value of Liver and Spleen Stiffness for Evaluation of Portal Hypertension in Compensated Cirrhosis. *Hepatol Commun* 2022; **6**: 950-964 [PMID: 34904404 DOI: 10.1002/hep4.1855]
- 25 Grama A, Pîrvan A, Sîrbe C, Burac L, Ștefănescu H, Fufezan O, Bordea MA, Pop TL. Extrahepatic Portal Vein Thrombosis, an Important Cause of Portal Hypertension in Children. *J Clin Med* 2021; **10** [PMID: 34207387 DOI: 10.3390/jcm10122703]
- 26 Senzolo M, Garcia-Tsao G, García-Pagán JC. Current knowledge and management of portal vein thrombosis in cirrhosis. *J Hepatol* 2021; **75**: 442-453 [PMID: 33930474 DOI: 10.1016/j.jhep.2021.04.029]
- 27 Takehara T, Sakamori R. Remaining challenges for the noninvasive diagnosis of esophageal varices in liver cirrhosis. *Esophagus* 2020; **17**: 19-24 [PMID: 31620917 DOI: 10.1007/s10388-019-00699-4]
- 28 Vuille-Lessard É, Rodrigues SG, Berzigotti A. Noninvasive Detection of Clinically Significant Portal Hypertension in Compensated Advanced Chronic Liver Disease. *Clin Liver Dis* 2021; **25**: 253-289 [PMID: 33838850 DOI: 10.1016/j.cld.2021.01.005]
- 29 Mandorfer M, Hernández-Gea V, García-Pagán JC, Reiberger T. Noninvasive Diagnostics for Portal Hypertension: A Comprehensive Review. *Semin Liver Dis* 2020; **40**: 240-255 [PMID: 32557480 DOI: 10.1055/s-0040-1708806]
- 30 Li J, Li J, Ji Q, Wang Z, Wang H, Zhang S, Fan S, Kong D, Ren J, Zhou Y, Yang R, Zheng H. Nomogram based on spleen volume expansion rate predicts esophagogastric varices bleeding risk in patients with hepatitis B liver cirrhosis. *Front Surg* 2022; **9**: 1019952 [PMID: 36468077 DOI: 10.3389/fsurg.2022.1019952]
- 31 Liu H, Sun J, Liu X, Liu G, Zhou Q, Deng J, Zhou J. Dual-energy computed tomography for non-invasive prediction of the risk of oesophageal variceal bleeding with hepatitis B cirrhosis. *Abdom Radiol (NY)* 2021; **46**: 5190-5200 [PMID: 34415412 DOI: 10.1007/s00261-021-03251-0]



Published by **Baishideng Publishing Group Inc**
7041 Koll Center Parkway, Suite 160, Pleasanton, CA 94566, USA

Telephone: +1-925-3991568

E-mail: bpgoftice@wjnet.com

Help Desk: <https://www.f6publishing.com/helpdesk>

<https://www.wjnet.com>

